Al Shaini and Blanco
Advances in Bridge Engineering (2023) 4:31
https://doi.org/10.1186/s43251-023-00110-4

Advances in
Bridge Engineering

ORIGINAL INNOVATION

Open Access

Bridge deck surface damage assessment using point cloud data

Issa Al Shaini[1*] and Adriana C. Trias Blanco[1]

*Correspondence:
alshaini.issa@gmail.com

[1] Civil and Environmental Engineering Department, Rowan University, Glassboro, NJ 08028, USA

Abstract

Bridge deck condition assessments are typically conducted through visual inspections and by incorporating traditional contact sensors for Non-Destructive Evaluation techniques such as hammer sounding and chain dragging, which require the keen expertise of trained inspectors. The accuracy of these inspections is proportional to the level of deterioration of the bridge deck, as the ability of the inspectors is correlated to the apparent level of damage. This study aims to improve the accuracy of bridge deck inspection processes by utilizing non-destructive evaluation techniques, including analyzing point cloud data gathered via Light Detection and Ranging (LiDAR) as a geometry-capturing tool for identifying surface irregularities. This research aims to evaluate and quantify the effectiveness and efficiency of LiDAR sensors in contributing to the suite of technologies available to perform bridge deck condition assessment. To achieve this, the research proposes to understand the deterioration pattern of New Jersey bridges, evaluate the results gathered from point cloud data collected on a full-scale bridge deck, and quantify the information gained from deploying LiDAR on operating bridges in New Jersey. Two data processing approaches were chosen to measure the gross and fine dimensions of the evaluated bridge decks, such as the Curvature Extraction and Slope Analysis method, and the Least Square Plane Fitting method, resulting in an accuracy of 97.92% in reference to the results gathered from reports generated through the analysis of state-of-the-art NDE technology data and visual inspection.

Keywords: Bridge deck, NDE, LiDAR, Point cloud, Condition assessment

1 Introduction

There are over 617,000 bridges in the United States. Currently, 42 percent of them are over 50 years old, and 7.5 percent, or 46,154, are in poor condition (ASCE, 2021); with the rapid deterioration pattern of bridge decks, implementing new reliable non-destructive evaluation (NDE) techniques is essential to maintain the structural health of reinforced concrete (RC) bridge decks by detecting early stages of deterioration and avoiding its continued detriment. Research done on bridge condition assessment shows that the use of point cloud data captured via Light Detection and Ranging (LiDAR) during construction (new or rehabilitation) can help to (a) estimate the location of the rebar

in the concrete deck by scanning during the construction stage (Abdelkhalek and Zayed 2020); (b) estimate rebar covers by comparing as-built scans to construction scans (Abu Dabous et al. 2017); and (c) locate low points on the deck's surface where water can sit by analyzing point cloud data (Alla and Asadi 2020). These aspects are critical factors in the performance of bridge decks, potentially causing early deterioration and shortening their service life.

Bridge inspection is addressed through visual inspections and advanced testing techniques. Visual inspections are typically executed by trained inspectors who search for deterioration in the form of cracks, steel corrosion, concrete spalling, section loss, deformations, and other deficiencies that can impact the structure's performance. Advanced testing techniques, such as non-destructive testing (NDT), complement visual inspections and provide more detailed information about the bridge's structural integrity. NDT methods include Ground Penetrating Radar (GPR), Half-cell Potential (HCP), and Electrical resistivity (ER) inspections. In recent years, new technologies such as LiDAR and drones have also been progressively used for bridge inspections, providing quantitative information on the bridge's condition and allowing for more efficient and accurate assessments. Overall, bridge inspections play a critical role in ensuring the safety and longevity of bridges, and continued advancements in inspection techniques and technologies are essential for maintaining the nation's infrastructure.

This research presents the results of an analysis performed on point cloud data of bridges in New Jersey, USA, demonstrating the applicability of LiDAR sensors for the condition assessment of bridge decks. The first phase of this study consisted of gathering point cloud data on eight (8) bridges in the same region, which had varying deck conditions ranging from 3 to 9 on a 0 to 9 scale. According to FHWA's Recording and Coding Guide for the Structure Inventory and Appraisal of the Nation's Bridges (FHWA 1995), concrete decks must be examined for cracking, scaling, spalling, leaching, chloride contamination, potholes, delamination, and full or partial depth failures before the structure is given a rating. Ratings of 0, 1, 2, 3, or 4 are associated with structurally poor; as condition 4 represents Poor, a rating of 3 depicts a Serious Condition, 2 means that the bridge deck is in a Critical Condition, 1 identifies as an Imminent Failure Condition, and 0 implies a Failed Condition; while a rating of 5–9 indicates that the bridge deck has some signs of deterioration but is generally in good condition with only minor defects or damage that do not require immediate attention; as 5 refers to a Fair Condition rating, 6 shows a Satisfactory Condition, 7 indicates Good Condition, 8 represents Very Good condition, and 9 signifies Excellent Condition. However, it is essential to note that even decks rated 5–9 require regular maintenance and monitoring to prevent further deterioration and ensure their continued safe operation.

The first phase of this research aimed to identify critical aspects that accurately predict deterioration rates and extend the bridge deck's service life. Low-rated decks were selected to prove the correlation between the bridge deck profile and the condition rating. At the same time, high-rated bridge decks were chosen to apply the knowledge gained from the deterioration correlation pattern. In the second phase, six (6) additional bridges in New Jersey were scanned to increase the reliability of the information gained and to develop a bridge deck deterioration trend based on Bridge Deck Characterization, a technique developed during this research. The common

factors between the bridges scanned were steel girders, concrete decks, single or continuous two-span configuration, and similar Average Daily Traffic (ADT) and Average Daily Truck Traffic (ADTT). These characteristics derive from an extensive literature review and analysis performed on historical bridge condition data, which allowed us to investigate further the deteriorating pattern of bridge decks in New Jersey. This data was extracted from the National Bridge Inventory (NBI) repository in the Infobridge website managed by the Federal Highway Administration (FHWA).

This research seeks to contribute to implementing point cloud data as a screening tool that can be rapidly deployed in combination with the suite of NDE techniques available for bridge deck inspection effectively and addressing early, efficient, qualitative, and quantitative bridge deck deterioration detection. A tool that can quickly and reliably generate point cloud data of targeted structures is the LiDAR sensor. LiDAR is a remote sensor that shoots beams of light to the evaluated object to create a 3D point cloud. The sensor uses the time it takes for the light beam to touch the object and return to the sensor, combined with the vertical and horizontal rotational angles of the scanner at the moment of emission, to calculate X, Y, and Z coordinates for each light pulse. Finally, combining the recorded points creates a point cloud of the scanned object. For this study, a FARO 150 S was used to collect the subject bridge's point cloud data for this case study. The operational processes of standard LiDAR scanners involve the emission of laser beams over a range of 300° (vertical) by 360° (horizontal) on a step with angular distances that can be as small as 0.009° (1.57E-4 rad), providing a maximum resolution of 111 points per degree angle. The scanner's precision is 1 mm in a 10 m range, and the effective range is 150 m (FARO 2021). The originated pulses bounce back from the object's surface to the scanner. Then, points are registered on a global coordinate system based on the pulses' time of flight and the vertical scanner's distance and horizontal rotational angles. Figure 1 shows (a) the operational principle of a typical LiDAR scanner, and (b) a sample of one of the concrete bridge decks scanned for the completion of this research.

LiDAR is also referred to as Laser Altimetry Detection and Ranging (LADAR), which, similarly, is a remote sensing technology that uses intense, focused beams of light to detect reflections and measures distance by estimating the time it takes for the beam of light to be emitted, bounce from the scanned surface, and return to the

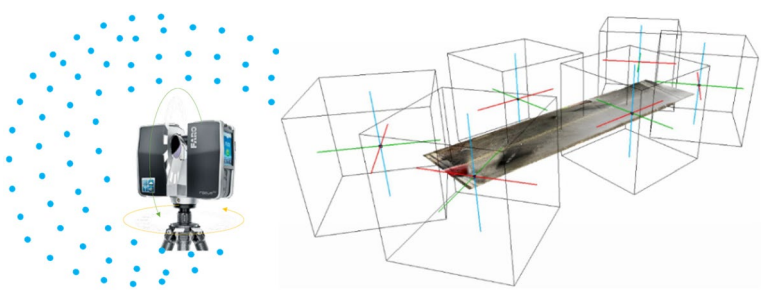

Fig. 1 **a** Operational principle of a LiDAR scanner; (**b**) Sample of a point cloud of a concrete bridge deck surface

scanner. In the same realm of technologies, Radio Detection and Ranging (RADAR) uses continuous radio waves instead of discrete laser light pulses.

2 Background

NDE technologies are used to detect potential damage or defects in concrete structures without causing any harm to the material itself. Each NDE technology has a unique physical concept that enables it to identify deficiencies. Half-cell potential (HCP) measures the electrochemical potential of reinforcing steel within the concrete to detect the early stages of corrosion (Elsener et al. 2003). Ground-penetrating radar (GPR) uses high-frequency electromagnetic waves to detect interfaces or discontinuities within the material, allowing engineers to locate features such as rebar, post-tensioning cables, and voids (Hugenschmidt and Loser 2008). Electrical resistivity (ER) measures the electrical resistivity of concrete to identify areas where the concrete may be weaker or more susceptible to damage (Chouteau and Beaulieu 2002). Impact echo (IE) generates stress waves within the evaluated member using a mechanical impact, which sensors can detect on the surface to determine the concrete's thickness and locate potential damage or defects (Scherr and Grosse 2021). Using these NDE techniques, engineers and technicians can select the appropriate method for a given application and interpret the results accurately to ensure the safety and longevity of concrete structures. Expanding modern NDE techniques can help mitigate some drawbacks of traditional inspection methods. A critical shortcoming of current NDE methods is the lack of geometry data available. The common practice combines NDE technologies with traditional measurement tools to reference collected data. This can be better addressed by implementing geometry capturing tools, such as LiDAR sensors, which can capture the external deterioration of elements, and their point cloud data can serve as a platform for the 3D representation of other information gathered via NDE methods. This research utilizes point cloud data captured via LiDAR as part of an NDE suite and the linking platform, ultimately serving as a predictive bridge deck condition assessment tool.

2.1 LiDAR for structural health monitoring of bridges

LiDAR has increasingly gained recognition for bridge structural health monitoring (SHM), focusing on characterizing the geometric features of components like girders and decks. One common application is to measure the vertical clearance under bridges to ensure safe passage for large vehicles (Kaartinen et al. 2022). LiDAR has also examined the relationship between environmental factors, loading, temperature, precipitation, and bridge deformation. Some studies have also employed LiDAR to detect structural damages, such as spalling and cracks. For instance, Teza et al. (2009) proposed an automated method for identifying mass loss in concrete bridges using a Terrestrial Laser Scanner (TLS), which involved three steps: (1) subdividing the point clouds into sub-areas; (2) applying Gaussian filtering and parabolic fitting to each point; and (3) classifying each sub-area as damaged or undamaged based on the curvature distribution. Researchers have investigated various uses of LiDAR technology for bridge evaluation and monitoring. One study used a phase-based laser system to compare distance and gradient-based methods for quantifying material loss in a bridge (Liu et al. 2010). Combining

these methods improved the capability of LiDAR for identifying and quantifying defects. Another study developed an automatic technique for measuring bridge clearance using TLS, which achieved millimeter-level accuracy (Liu et al. 2012). While Watson et al. (2012), evaluated the impact of various parameters on bridge clearance measurements using periodic TLS scans, while Liu & Chen (2013) assessed the applicability and reliability of LiDAR for bridge health monitoring through sensitivity analyses on a full-scale bridge, including tests of range measurement ability, the accuracy of the scanner, and automatic inspection algorithms.

In a study by Riveiro et al. (2013), a method was introduced for measuring the minimum vertical clearance of bridges and obtaining the profile of prestressed concrete beams using photogrammetry and TLS surveys. To estimate the vertical clearance and beam cambers, a 3D curve-fitting algorithm was developed, which achieved high statistical correlation coefficients when implemented on a full-scale bridge. Geometrical information of bridges, including elevation, span length, girder spacing, bottom flange width, and web height, was recorded by a LiDAR (Dai et al. 2014), and the girder deflections were calculated by comparing the girder elevation coordinates of the scans with and without truck weight. The proposed approach proved more accurate and accessible than contact methods, even in estimating the bridge's natural frequencies. In addition, a fully automated TLS point cloud segmentation procedure was developed by Riveiro et al. (2016) for the SHM of masonry arch bridges. The proposed algorithm used a voxelization process to filter out redundant data and used topological constraints to establish individual structural elements' spatial relation and order. An automated processing method of point cloud data applied for SHM of masonry arch bridge piers suggested that the algorithm showed coherent results with minor issues due to poor point cloud quality when tested on five datasets. They segmented a full-scale bridge into its structural components and identified structural faults by analyzing the geometric parameters of pier faces and their topological relationship with other bridge elements.

SHM technology for masonry bridges using TLS data and GPR was presented by Pérez et al. (2018), where they compared TLS measurements with historical drawings to identify anomalies in hyperbolic reflections and determine the bridge filling configuration. Ziolkowski et al. (2018) introduced a TLS-based framework for detecting structural deformation in composite footbridges. They generated two mesh models using the Fast-Marching algorithm and compared them to check for changes after applying a load to the bridge. Kim et al. (2018) investigated a crack identification and quantification approach for concrete structures using unmanned aerial vehicles (UAV). They generated a point cloud-based background model of the structure, applied convolutional neural networks to high-resolution images for crack detection, and used transfer learning from 384 crack images for classification and localization on a full-scale bridge. Cha et al. (2019) proposed a deflection and deformation measurement application for bridges using a shape information model constructed from the improved octree data structure and TLS data, where the deflection was estimated based on the octree space division and validated using linear variable differential transformer (LVDT). The research developed a new bridge inspection technique using UAV imagery point clouds, constructing a triangular mesh and density map to reduce errors in data. The iterative closest-point

algorithm was applied with TLS data to measure thickness, point distribution, and point-to-point distances for a full-scale bridge.

Lee et al. (2019) introduced a reflector-based framework for measuring long-term bridge displacement using LiDAR. The framework included a reflector positioning strategy, measuring the reflector coordinates, and calculating the displacement. The proposed method was validated through the test of a prestressed concrete bridge. Liu. et al. (2019) used TLS to construct a Digital Surface Model and identify the potential damage area of a bridge. Ground-based microwave interferometry was used to confirm the damage, and interferometry synthetic aperture radar (INSAR) was applied to analyze the causes of the damage to a full-scale bridge. Bolourian and Hammad (2020), introduced a 3D path-planning technique for LiDAR-equipped UAVs to inspect bridges, involving three steps: (1) assigning essential values based on the moment and shear force values from structural analysis, (2) selecting Viewpoints of Interest for perpendicular and overlapping views, and (3) calculating the optimal collision-free path using a Genetic Algorithm and A* algorithm. After testing on a full-scale bridge, the method reduced flight time, processing time, and workload while enhancing visibility, reliability, and accuracy. Erdélyi et al. (2020), developed a deformation monitoring method using TLS and ground-based radar interferometry data, which was also tested on a full-scale bridge. By comparing the two methods, the authors found similar results. Cha et al. (2020), proposed a displacement estimation method for bridge structures using four laser scanning-based techniques. The method involved rearranging points in a 3D space and creating nodes to calculate the displacement. The proposed method reduced the time required for displacement estimation but increased data processing time compared to other approaches.

The literature review analysis presents how point cloud data captured via LiDAR is progressively being incorporated as an NDE technology that, with the use of state-of-the-art methods and algorithms, can be implemented to assess the condition of primary structural bridge components such as girders and, for measuring large- and small-scale dimensions to assess the condition and integrity of the overall structure. Yet, there is a persistent knowledge gap that would increase the reliability of using point cloud data for assessing bridge decks, which refers to the relationship between deformations and damages found on the element's surface with its internal condition. Hence, the decision to pursue this research project.

2.2 Validation testbed

A fully instrumented, full-scale bridge was chosen to collect information as a validation dataset. Detailed information on the results gathered from the full-scale bridge is presented in the following section. The specimen is the 50-foot single-span bridge tested in the Bridge Evaluation and Accelerated Structural Testing (BEAST) lab at Rutgers University. The tested specimen, which is deteriorated under a controlled environment (load, temperature, humidity), is instrumented with strain gauges, displacement gauges, accelerometers, and internal humidity sensors. The specimen was subjected to a series of inspections along the test. NDE data was collected (e.g., HCP, GPR, IE) to correlate the results to the amount of deterioration imposed. In addition, LiDAR was deployed to capture the deteriorated condition at each inspection performed.

This test specimen consisted of four steel-rolled beams of W27 × 84, covering a total span of 14,61 m (47ft-11 ¼in). The four lines of diaphragms were composed of C15 × 33.9 sections. On top of the girders, a haunch that varied from 2,54 cm (1 in.) deep at Abutment 1 (fixed end) to 7,62 cm (3 in.) deep at Abutment 2 (expansion end) received the concrete deck, which had a total length of 15,27 m (50ft-1 ¼in) and an out-to-out width of 8,23 m (27ft.). Two curbs of 43,815 cm (1ft-5 ¼ in) wide by 15,24 cm (6 in.) deep ran along the top outside edges of the deck, leaving a curb-to-curb distance of 7,35 m (24ft-1 ½ in). The BEAST test specimen was subjected to continued deterioration inside the lab's chamber, including live load cycling, freeze–thaw, and brine water spray. Figure 2 presents a point cloud of the BEAST lab with the bridge specimen on an elevation heat map. The NDE data collection was performed throughout the length of the test at different deterioration stages. LiDAR data was collected: (a) during the construction of the bridge, recording the as-built dimensions, (b) during an intermediate deterioration stage, and (c) at the end of the first phase of the BEAST specimen project.

3 Methodology

It was hypothesized that the deterioration stage of bridge decks is correlated to the damage observed on the deck's surface. Therefore, the condition rating could be determined based on the characterization of the state of damage. To ensure a successful project, the team took the following steps: (1) literature review: since the facilities used for the validation data set involved the analysis of a full-scale single-span steel-girder bridge, the literature review focused on the deterioration patterns of steel girder bridge decks to minimize the number of variables; (2) condition assessment of a full-scale bridge deck deteriorated in a controlled environment: the Bridge Evaluation and Accelerated Structural Testing (BEAST) lab at Rutgers University's Center for Advanced Infrastructure and Transportation (CAIT) facility was performing the accelerating testing, through the implementation of traditional non-destructive evaluation (NDE) methods such as HCP, GPR, ER, USW, IE, and the addition of point cloud data captured via terrestrial LiDAR; (3) scanning via terrestrial LiDAR of bridge

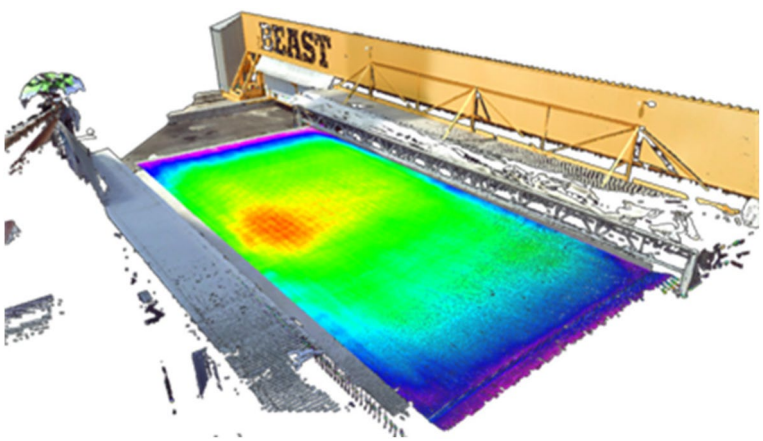

Fig. 2 Point Cloud of the BEAST bridge specimen

decks in New Jersey to evaluate the potential correlation and applicability of the proposed approach; (4) implementation of two point cloud data processing methods to quantify the areas of damage; (5) comparison of the results gathered from the New Jersey bridges with the trend found on the validation data set.

4 Overview of the data processing methods

The point cloud data collection methodology consisted of placing the scanner at different locations surrounding the bridge specimen to capture the deck's surface. Then, the scans are registered through the scanner's software, Faro SCENE; this process was performed by referencing targets (white spheres 23 cm in diameter) placed at strategic locations during data collection and through superposing the plan view of the point cloud. The registered point cloud data was processed and analyzed using software tools such as CloudCompare and Excel through two different approaches that allowed to characterize the geometry of the deck: (a) Curvature Extraction and Slopes Analysis, and (b) Least Square Method Plane Fitting. The results analysis can identify low points on the bridge deck surface where water can accumulate, which allows maintenance and repair operations to be planned.

4.1 Curvature Extraction and Slope Analysis (CESA) method

This project evaluated the presence of various aspects using the point cloud data collected for each bridge deck. These aspects include: (a) Rutting percentage: expressed as a percentage of the deck's total area and indicate the extent of rutting; (b) Percentage of overall potholes: expressed as a percentage of the deck's total area and indicate the extent of potholes; (c) Section loss at joint locations: expressed as a percentage of the deck's area and indicate the amount of section loss at the joints; (d) Longitudinal curvature: each deck will be analyzed to determine whether there is a correlation between low points in the deck and the condition stage; and I Transverse curvature: the transverse slope will be compared to the evaluate the presence of the recommended 2% slope on the bridge decks and ensure proper water drainage. Figures 3, 4 and 5 show where the longitudinal and transverse cross sections were taken from the testbed bridge deck. This approach was taken to better visualize the d'ck's curvature, first explored and analyzed through the elevation heat map in Fig. 3. The CESA was applied to all the bridge decks

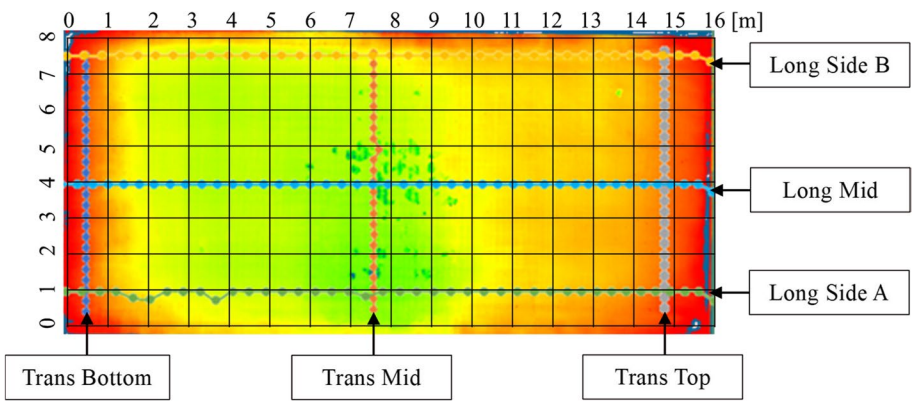

Fig. 3 Plan view of the testbed and location of transverse and longitudinal cross-sections

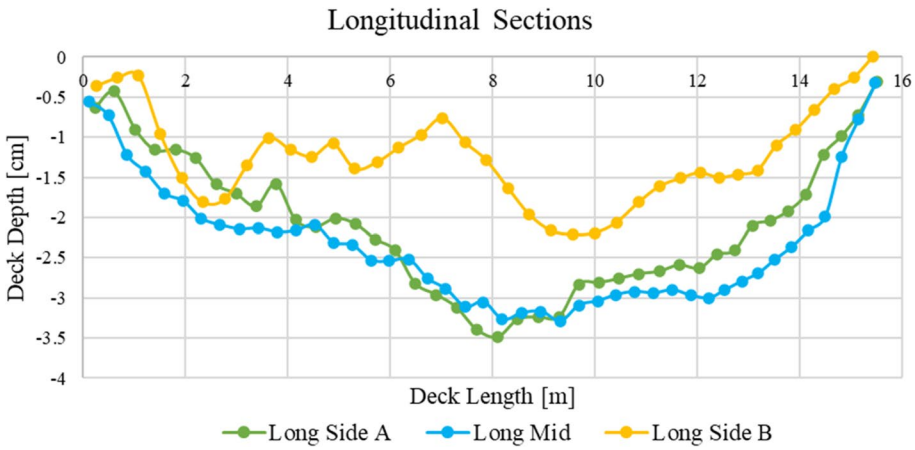

Fig. 4 Deck's longitudinal sections

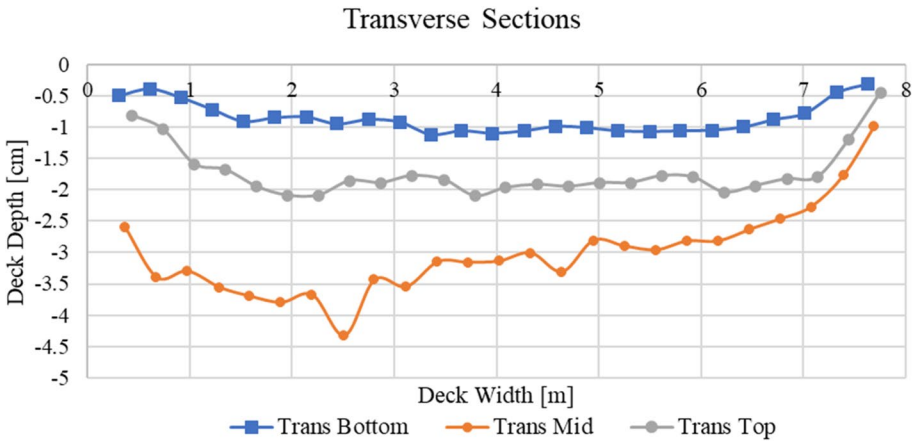

Fig. 5 Deck's transverse sections

evaluated in this study. To produce the information presented in Figs. 4 and 5, three longitudinal lines were selected: one near the left edge ("Side B"), one at mid-section, and one near the right edge ("Side A"), and three transverse lines were selected: one near the southern support ("Bottom"), one at mid-span, and one near the northern support ("Top"). The distance between the data points was set to approximately 0.40 m. A plan view of these lines are presented in Fig. 3 to facilitate their reference within the deck.

The longitudinal sections presented in Fig. 4, demonstrate the curvature of the profile of the bridge deck. A low region is present at midspan, especially in sections *Long Mid* and *Long Side A*, which is an area that potentially serves for water to sit longer due to its inability to run off the deck. The same analysis can be drawn from the transverse curvature shown in Fig. 5, where the bridge deck presents flat and concave sections, with a deeper depression in the *Trans Mid* section. The geometry data presented above, and throughout this research is possible given that the point cloud data generated via a LiDAR sensor, provided X, Y, and Z coordinates of each data point.

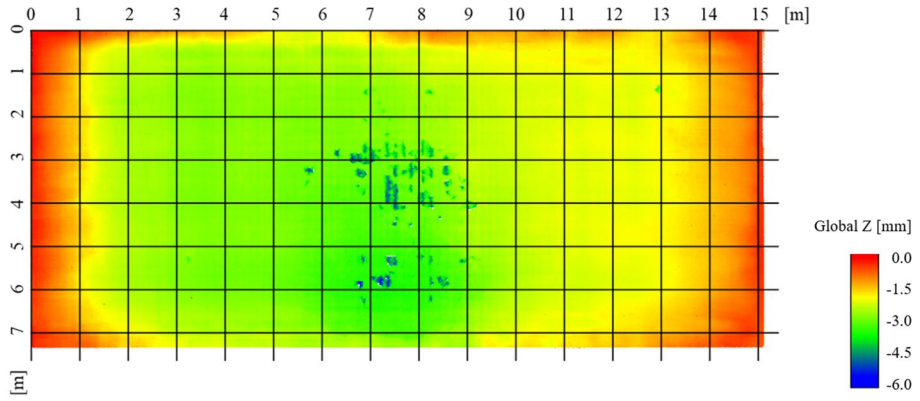

Fig. 6 Plan view of the deck by elevation

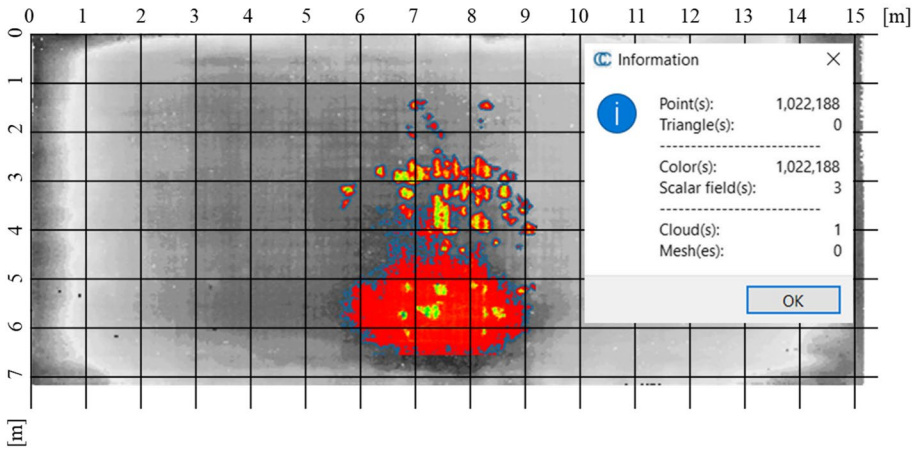

Fig. 7 Isolated damaged area representing 1,022,188 points

4.2 Least Square Plane Fitting (LSPF) method

After analyzing the curvature and slope of the deck, where multiple cross-sections were evaluated, a second data analysis approach was taken to better characterize the damage condition. For this, horizontal projections and plane fitting were completed, showing areas of interest where distances from the fitted planes were -36 mm (-1.4 in.) below the fitted planes, indicating an accentuated depression. Figure 6 presents an elevation heat map of the deteriorated testbed bridge deck (data collection date: 10 Oct., 2022), where it is clear that potholes were already developing on the surface of the deck. Once this potentially damaged area was isolated, the points below -6 mm (-0.24 in.) were highlighted and classified as actual damage. This criterion assumes that the surface roughness of a concrete bridge deck is between 3 and 5 mm (0.16 in.), then a surface irregularity of 6 mm would represent approximately two times the roughness. Figure 7 compares the study area, highlighting the points classified as damaged.

(a) (b)

Fig. 8 Visual inspection images from the inspection reports of the testbed (**a**) Small to large spalls looking east 3,25 m2 (35 sq.ft.); (**b**) large spalls looking south 2,32 m2 (25 sq.ft.)

Table 1 Bridge deck (58) Visual inspection report from the BEAST Bridge Inspection reports indicating damages

RATING	COMPONENT	REMARKS
5	Wearing Surface	(1/2″ Integral wearing surface) One large area of moderate scaling near the mid-span east half of the deck (180 SF). Some minor scaling at random locations (30 SF). Some pop-outs and insignificant cracking at random locations
5	Top of Deck	Some deep spalls (> 1″), mostly with exposed rebar near the mid-span of the deck (35 SF total)
8	Underside of Deck	Bay 1: SIP forms with isolated rust along the connection to the top flange of the girder. Bays 2 & 3: Reinforced concrete with no significant defects

5 Test specimen results

5.1 Visual inspection Vs. Point cloud data

The Visual Inspection regarding the results presented in this section was obtained during the same testing cycle when the point cloud data was collected; therefore, both inspection methods correspond to the same deterioration stage of the deck. The inspection reports obtained for the testbed showed that the deck had a condition rating of 5 (Fair). This classification was reported as a total area of damage of 3,25 m2 (35 sq.ft.) of spalls equal to or deeper than 2,54 cm (1 in.) or > 15,24 cm (> 6 in.) in diameter. The images from the Visual Inspection report captured in July 2021 can be seen in Fig. 8. Even though Fig. 8 shows water on top of the deck's surface, this water was removed to perform point cloud data collection, since the LiDAR scanner utilized for this inspection cannot pass through water, which would alter the resu'ts' quality.

A summary of the inspection report for the testbed deck condition rating can be seen in Table 1. This table indicates the amount of damaged area identified during the visual inspection. Where the level of damage is indicated and described for each condition rating (e.g., spall > 2,54 cm (> 1 in.)). The testbed has a 7.35 m × 15.27 m deck forming a total area of 112.23 m2 (1208.03 sq.ft.). Even though the underside of the deck was evaluated during Visual Inspection, Point Cloud data was not collected as the proj'ct's objective focuses on evaluating the deck's surface. Thus, further analysis was conducted between both inspection methods concerning the deck's underside.

The analysis of the validation testbed was conducted on a specific area of the bridge deck identified as the area of interest due to its progressive damage and concaved surface identified in previous scans. The analysis was focused on comparing the damaged location assessed via visual inspection (e.g. inspection reports), which indicated

3,25 m2 (35 sq.ft.) of damage on the top of the deck of spalls > 2,54 cm (> 1 in.) deep or > 15.24 cm (> 6 in.) in diameter; which from the total area of the deck, equivalent to 111,02 m2 (1195 sq.ft.), represent 2.93% of area of damage. The results of the point cloud analysis showed a total of 1,022,188 points identified as damaged points out of the 36,085,551 points in the entire bridge deck's point cloud, which indicates that the damage represents 2.83% of the bridge d'ck's total area, or 3,14 m2 (33.81 sq.ft.), a 96.6% accuracy when compared to the assessment made through visual inspection. These results suggest that the analysis of the testbed is a reliable method for identifying and quantifying damage on bridge decks. A summary of these results is presented in Table 2.

The percent of damage of each inspection method was calculated by dividing the area or points corresponding to the identified damage by the area or points corresponding to the total surface of the deck. Equation (1) was used to relate the percent of damage identified via PC to the one reported on the VI.

$$PC\ Vs.\ VI = \frac{Point\ Cloud\ Percent\ of\ Damage}{Visual\ Inspection\ Percent\ of\ Damage} \times 100 \tag{1}$$

5.2 Non-destructive evaluation vs. Point cloud data

This research utilized the information gathered from the BEAST Laboratory test specimen to validate the results from point cloud data captured via LiDAR. This comparison allowed us to understand the correlation between internal element transformation and external symptoms of the bridge deck due to the continued deterioration. The development of clear correlation trends was possible given the amount of NDE data available at different deterioration stages of the test specimen. By comparing the Point Cloud results with the inspection reports for the test specimen, we demonstrated the data's accuracy and the potential for this approach as a screening tool to reduce the need for the immediate costly deployment of a suite of technologies that would also cause traffic disruption.

A detailed analysis of the comparison of the suite of NDE data collected from the testbed versus the point cloud data captured via LiDAR was performed to correlate the internal damage detected from the non-destructive evaluation technologies and the external changes in geometry on the top surface of the bridge deck. Table 3 summarizes the results gathered from the test performed, including half-cell potential (HCP), ground penetrating radar (GPR), electrical resistivity (ER), ultrasonic wave (USW), impact echo (IE), and point cloud captured via LiDAR.

Table 2 Summary of visual inspection Vs. Point cloud data analysis

Inspection method	Deck area or points	Damaged area or points	Percent of damage
Visual Inspection (VI)	112.23 m2	3,25 m2	2.89%
Point Cloud (PC)	36,085,551 points	1,022,188 points	2.83% (97.92% of visual inspection)

Table 3 NDE and point cloud data collected from the BEAST specimen

NDE	2019 – 07 – 30 (construction)	2021 – 02 – 24	2021 – 07 – 21	Scale & Units
HCP	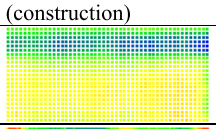	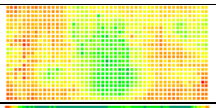	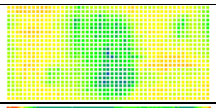	135.0 -620.0 (mV)
GPR (top cover)	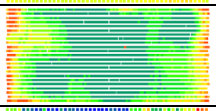	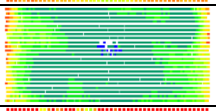	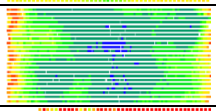	7.6 3.8 0.0 (cm)
ER	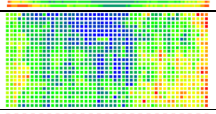	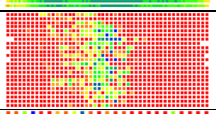	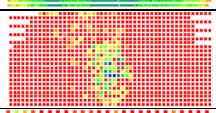	5.0 1.1 (KΩ.cm)
USW	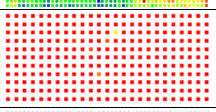	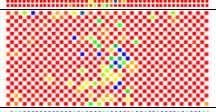	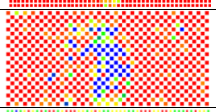	4500 3000 (ksi)
IE	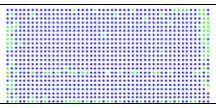	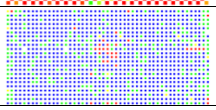	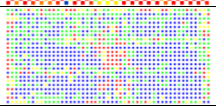	4 1 (index)
LiDAR (elevation)	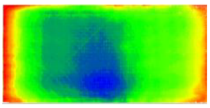	Not available	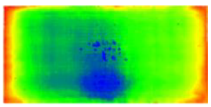	0 3.5 -4.5 (cm)
Deck's B/W Image		Not available	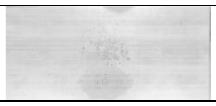	NA

Table 3 indicates that the point cloud data was the only NDE capable of detecting an anomaly in the geometry of the bridge deck from the first set of scans. GPR data correlates to the point cloud data, indicating a shallow top cover for the reinforcing steel. However, this data does not directly indicate a depression at midspan as it could indicate an issue with the rebars instead, leaving point cloud data as the only clear evidence of the localized anomaly of the surface of the bridge deck. The NDE data collected on February 24th, 2021, and July 21st, 2021, clearly evidenced deterioration in the bridge deck, which originated around midspan, as predicted, given the depression of the bridge deck detected by point cloud data analysis.

6 Evaluation of operating bridges in new Jersey

Based on the information gained from studying the NDE and point cloud data captured from the full-scale bridge deck specimen, this section presents the evaluation of 13 operating bridges in New Jersey, USA, incorporating the results found from the testbed evaluation. Figure 9 shows a map of New Jersey with the location of the evaluated bridge decks. A terrestrial LiDAR was deployed during a regular operating environment, allowing the point cloud data to capture the undisturbed condition of the decks. Once the point cloud data of each bridge deck was registered, the same analysis procedures, CESA and LSPF, were taken to analyze each structure. Table 4 summarizes the information collected from such analysis, and Fig. 10 presents a graph relating the deck's condition rating to the percent of damage found via LSPF analysis.

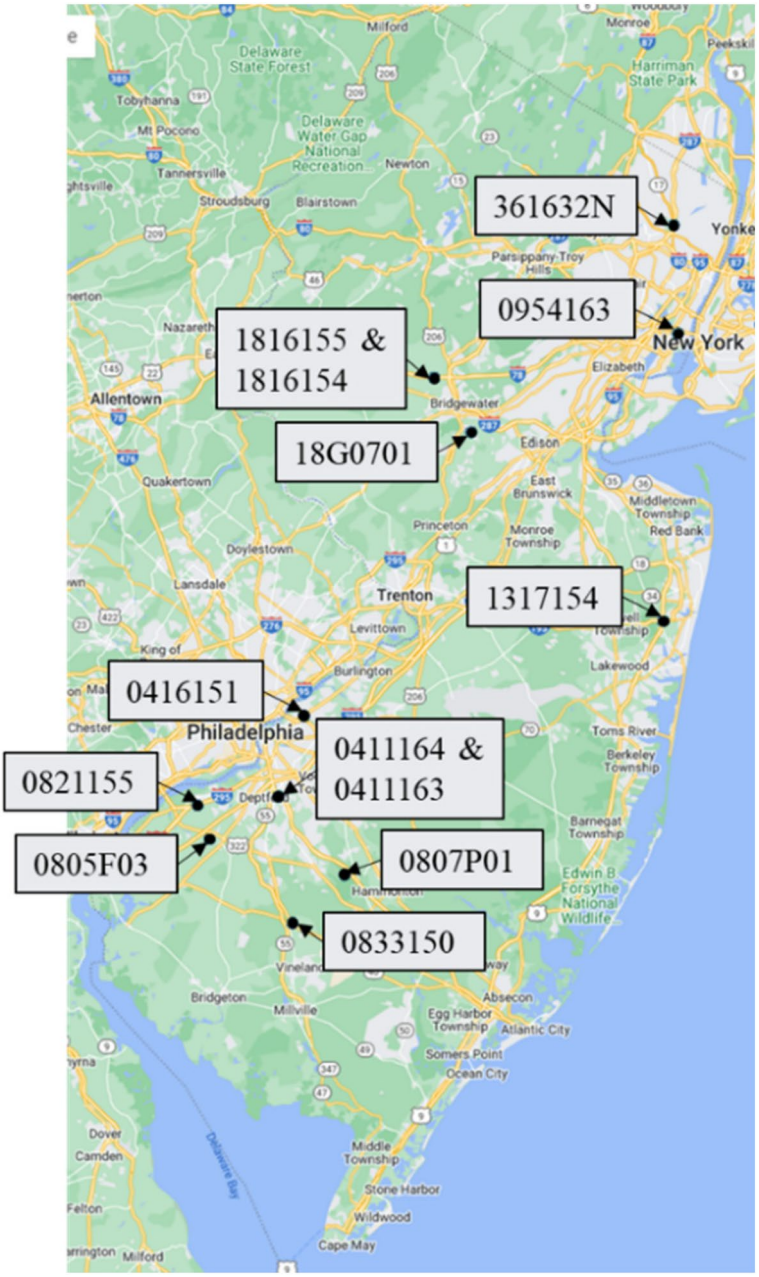

Fig. 9 Bridge decks evaluated in the state of New Jersey

The trend found in Fig. 10 evidences a correlation between the deck's condition rating and the level of damage found on the top surface. This graph includes the thirteen bridge decks from NJ and the testbed from the BEAST Laboratory.

Table 4 Damage percentage analysis through least square plane fitting results

Bridge #	Deck condition	Deck points	Damaged points	Percentage of damage
1816155	3	521055	26396	5.07%
0954163	4	9676590	370815	3.83%
0416151	4	10948500	430004	3.93%
0411163	5	10566997	287096	2.72%
Testbed	5	36085551	1022188	2.83%
1816154	6	2730714	68766	2.52%
0805F03	6	1.05E + 08	2731256	2.60%
361632N	8	97715013	1277123	1.31%
0411164	8	11543083	230851	2.00%
1317154	7	50058036	1099241	2.20%
0807P01	7	23976488	581585	2.43%
0833150	7	12119792	285037	2.35%
0821155	9	3340916	36018	1.08%
18G0701	9	1614190	18774	1.16%

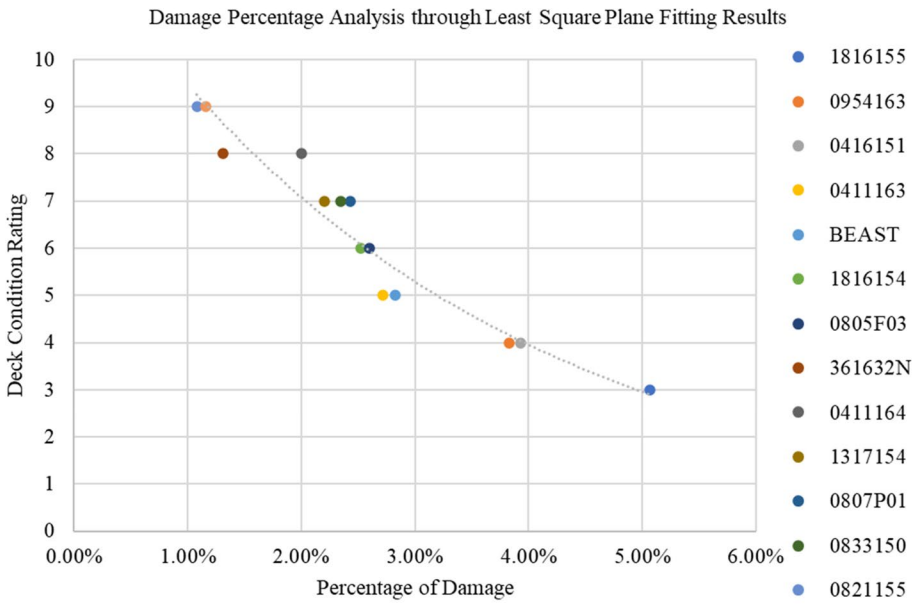

Fig. 10 Condition rating vs. Percent of Damaged

7 Conclusions

Based on the analysis of the NDE and LiDAR data, it was found that the condition rating of bridge decks can be correlated with the percentage of damaged surface area. This correlation was established by comparing the results obtained from scanning operating bridges in New Jersey with the test bridge. By establishing this correlation, it was possible to develop a deterioration trend that can be used to prioritize bridge inspections and maintenance efforts.

The findings of this research have significant implications for bridge maintenance and repair operations. By utilizing LiDAR technology, particularly the methods developed and implemented in the research: the Curvature Extraction and Slope Analysis

(CESA) method; and the Least Square Plane Fitting (LSPF) method, as part of the suite of a non-destructive evaluation techniques, it is possible to accurately assess the health of bridge decks and predict their future deterioration rates. This information can be used to develop strategies to extend the service life of bridges, prioritize repair and maintenance efforts, and effectively manage limited resources.

This research has demonstrated the effectiveness of LiDAR scanning for evaluating the condition of operating bridges in New Jersey and establishing a correlation between deck condition rating and the percentage of damaged surface area. The results obtained from this study provide valuable insights into the deterioration trend of bridge decks and highlight the potential of LiDAR technology as a reliable tool for bridge assessment and maintenance planning. Further research and scanning of more bridges can enhance the accuracy and reliability of the established deterioration trend, contributing to the development of robust strategies for preserving the structural health of bridge decks and ensuring the safety and longevity of bridge infrastructure.

LiDAR proved its efficiency as a geometry-capturing tool for bridges' decks. The future goal through further studies and analysis is to deploy Terrestrial Lidar Scanning TLS as a screening tool to be included in the suite of NDE techniques to address early bridge deck deterioration and perform a cost analysis that can provide tangible results on budget management.

Abbreviations

ASCE	American Society of Civil Engineering
ADT	Average Daily Traffic
ADTT	Average Daily Truck Traffic
BEAST	Bridge Evaluation and Accelerated Structural Testing
CESA	Curvature Extraction and Slope Analysis
ER	Electrical Resistivity
FHWA	Federal Highway Administration
GPR	Ground Penetrating Radar
HCP	Half-cell Potential
IE	Impact Echo
LSPF	Least Square Plane Fitting
LiDAR	Light Detection and Ranging
NBI	National Bridge Inventory
NDE	Non-destructive Evaluation
NDT	Non-destructive Testing
USW	Ultrasonic Waves

Acknowledgements
The authors acknowledge the support of Rutgers University Center for Advance Infrastructure and Transportation (CAIT) as part of the University Transportation Centers (UTC) for providing the funds and facilities needed to complete this research.

Authors' contributions
The authors confirm their contribution to the paper as follows: study conception and design: Issa Al Shaini and Dr. Adriana Trias; data collection: Issa Al Shaini and Dr. Adriana Trias; analysis and interpretation of results: Issa Al Shaini and Dr. Adriana Trias; draft manuscript preparation: Issa Al Shaini, and Dr. Adriana Trias. All authors reviewed the results and approved the final version of the manuscript.

Funding
This project was funded through the Rutgers University Center for Advance Infrastructure and Transportation (CAIT) as part of the University Transportation Centers (UTC).
University Transportation Centers,69A3551847102

Availability of data and materials
The point cloud data used for this research can be found at https://osf.io/yt5jn/files/osfstorage.

Declarations

Competing interests
There are no competing interests to declare.

Received: 25 August 2023 Accepted: 25 October 2023
Published online: 03 December 2023

References

Abdelkhalek S, Zayed T (2020) Comprehensive inspection system for concrete bridge deck application: current situation and future needs. J Perform Constr Fac 34(5):03120001. https://doi.org/10.1061/(asce)cf.1943-5509.0001484
Abu Dabous S, Yaghi S, Alkass S, Moselhi O (2017) Concrete bridge deck condition assessment using IR thermography and ground penetrating radar technologies. Autom Constr 81:340–354. https://doi.org/10.1016/j.autcon.2017.04.006
Alla S, Asadi SS (2020) Integrated methodology of structural health monitoring for civil structures. Mat Today: Proc 27:1066–1072. https://doi.org/10.1016/j.matpr.2020.01.435
ASCE (2021) Infrastructure Report Card. https://infrastructurereportcard.org/wpcontent/uploads/2020/12/National_IRC_2021-report.pdf
Bolourian N, Hammad A (2020) Lidar-equipped UAV path planning considering potential locations of defects for bridge Inspection. Autom Constr 117:103250. https://doi.org/10.1016/j.autcon.2020.103250
Cha G, Park S, Oh T (2019) A terrestrial LIDAR-based detection of shape deformation for maintenance of bridge structures. J Constr Eng Manage 145(12):04019075. https://doi.org/10.1061/(asce)co.1943-7862.0001701
Cha G, Sim S-H, Park S, Oh T (2020) Lidar-based bridge displacement estimation using 3D spatial optimization. Sensors 20(24):7117. https://doi.org/10.3390/s20247117
Chouteau M, Beaulieu (2002) An Investigation on Application of the Tomographic Resistivity Method to Concrete Structures. Presented at the 2nd International Conference on the Application of Geophysical and NDT Methodologies to Transportation Facilities and Infrastructure, Los Angeles, Calif
Dai K, Boyajian D, Liu W, Chen S-E, Scott J, Schmieder M (2014) Laser-based field measurement for a bridge finite-element model validation. J Perform Constr Fac 28(5):04014024. https://doi.org/10.1061/(asce)cf.1943-5509.0000484
Elsener B, Andrade C, Gulikers J, Polder R, Raupach M (2003) Half-cell potential measurements—Potential mapping on reinforced concrete structures. Mater Struct 36(7):461–471
Erdélyi J, Kopáčik A, Kyrinovič P (2020) Spatial Data Analysis for Deformation Monitoring of Bridge Structures. Appl. Sci 10:8731. https://doi.org/10.3390/app10238731
FARO. (2021). 3D measurement, imaging & realization solutions. FARO.com. Retrieved from https://www.faro.com/
FHWA (1995) (rep.) The recording and coding guide for the structure inventory and appraisal of the Nation's bridges. Office of Engineering, Office of Engineering, Washington
Hugenschmidt J, Loser R (2008) Detection of chlorides and moisture in concrete structures with ground penetrating radar. Mater Struct 41:785–792
Kaartinen E, Dunphy K, Sadhu A (2022) LIDAR-based structural health monitoring: applications in civil infrastructure systems. Sensors 22(12):4610. https://doi.org/10.3390/s22124610
Kim I-H, Jeon H, Baek S-C, Hong W-H, Jung H-J (2018) Application of crack identification techniques for an aging concrete bridge inspection using an unmanned aerial vehicle. Sensors 18(6):1881. https://doi.org/10.3390/s18061881
Lee J, Lee KC, Lee S, Lee YJ, Sim SH (2019) Long-term displacement measurement of bridges using a lidar system. Struct Contr Health Monitor 26(10):2428. https://doi.org/10.1002/stc.2428
Liu W, Chen S (2013) Reliability analysis of bridge evaluations based on 3D light detection and ranging data. Struct Control Health Monit 20(12):1397–1409. https://doi.org/10.1002/stc.1533
Liu W, Chen S, Hauser E (2010) Lidar-based bridge structure defect detection. Exp Tech 35(6):27–34. https://doi.org/10.1111/j.1747-1567.2010.00644.x
LiuChenHasuer WSEE (2012) Bridge clearance evaluation based on terrestrial LIDAR SCAN. J Perform Constr Facil 26(4):469–477. https://doi.org/10.1061/(asce)cf.1943-5509.0000208
Liu X, Wang P, Lu Z, Gao K, Wang H, Jiao C, Zhang X (2019) Damage detection and analysis of urban bridges using Terrestrial Laser Scanning (TLS), ground-based microwave interferometry, and permanent scatterer interferometry synthetic aperture radar (PS-Insar). Remote Sensing 11(5):580. https://doi.org/10.3390/rs11050580
Pérez J, de Sanjosé Blasco J, Atkinson A, del Río Pérez L (2018) Assessment of the structural integrity of the Roman Bridge of Alcántara (Spain) using TLS and GPR. Remote Sensing 10(3):387. https://doi.org/10.3390/rs10030387
Riveiro B, González-Jorge H, Varela M, Jauregui DV (2013) Validation of Terrestrial Laser Scanning and photogrammetry techniques for the measurement of vertical underclearance and beam geometry in structural inspection of Bridges. Measurement 46(1):784–794. https://doi.org/10.1016/j.measurement.2012.09.018
Riveiro B, DeJong MJ, Conde B (2016) Automated processing of large point clouds for structural health monitoring of masonry arch bridges. Autom Constr 72:258–268. https://doi.org/10.1016/j.autcon.2016.02.009
Scherr JF, Grosse CU (2021) Delamination detection on a concrete bridge deck using impact echo scanning. Struct Concr 22(2):806–812. https://doi.org/10.1002/suco.202000415
Teza G, Galgaro A, Moro F (2009) Contactless recognition of concrete surface damage from laser scanning and curvature computation. NDT and E Int 42(4):240–249. https://doi.org/10.1016/j.ndteint.2008.10.009
Watson C, Chen S-E, Bian H, Hauser E (2012) Three-dimensional terrestrial LIDAR for operational bridge clearance measurements. J Perform Constr Facil 26(6):803–811. https://doi.org/10.1061/(asce)cf.1943-5509.0000277
Ziolkowski P, Szulwic J, Miskiewicz M (2018) Deformation analysis of a composite bridge during proof loading using point cloud processing. Sensors 18(12):4332. https://doi.org/10.3390/s18124332

Publisher's Note